Mean force on a finite-sized spherical particle due to an acoustic field in a viscous compressible medium

Subramanian Annamalai, S. Balachandar,* and Manoj K. Parmar
Department of Mechanical and Aerospace Engineering, University of Florida, Gainesville, Florida 32611, USA
(Received 20 January 2014; published 12 May 2014)

An analytical expression to evaluate the second-order mean force (acoustic radiation force) on a finite-sized, rigid, spherical particle due to an acoustic wave is presented. The medium in which the particle is situated is taken to be both viscous and compressible. A far-field derivation approach has been used in determining the force, which is a function of the particle size, acoustic wavelength, and viscous boundary-layer thickness. It is assumed that the viscous length scale is negligibly small compared to the acoustic wavelength. The force expression presented here (i) reduces to the correct inviscid behavior (for both small- and finite-sized particles) and (ii) is identical to recent viscous results [M. Settnes and H. Bruus, Phys. Rev. E **85**, 016327 (2012)] for small-sized particles. Further, the computed force qualitatively matches the computational fluid dynamics (finite-element) results [D. Foresti, M. Nabavi, and D. Poulikakos, J. Fluid Mech. **709**, 581 (2012)] for finite-sized particles. Additionally, the mean force is interpreted in terms of a multipole expansion. Subsequently, considering the fact that the force expansion is an infinite series, the number of terms that are required or adequate to capture the force to a specified accuracy is also provided as a function of the particle size to acoustic wavelength ratio. The dependence of the force on particle density, kinematic viscosity, and bulk viscosity of the fluid is also investigated. Here, both traveling and standing waves are considered.

DOI: 10.1103/PhysRevE.89.053008 PACS number(s): 47.55.Kf, 43.35.+d, 47.61.Jd

I. INTRODUCTION

Particles, when subjected to an acoustic field, experience a net force. While in the linear approximation the time-average force is identically zero, the second-order terms on time averaging survive and impart a mean force on the particle. Although orders of magnitude smaller than the first-order quasisteady drag, the second-order force is used in a wide variety of applications including microfluidics, pharmaceutical industries, biomedicine, and microgravity, to name a few.

The study of this mean force (widely referred to as acoustic radiation force in the literature) involves three relevant length scales: R, the radius of the particle; λ, the wavelength of the acoustic field; and δ, the viscous (Stokes) length scale of the diffused momentum. The past work can be presented in terms of the above length scales. King [1] derived an expression for the radiation force experienced by a rigid sphere suspended in an inviscid medium where $\delta \to 0$. He simplified this expression to account for particle sizes much smaller than the wavelength and calculated the mean second-order force on a sphere subjected to plane traveling and standing waves. A complete solution for the force due to plane stationary and quasistationary waves for a finite-sized particle (ratio of particle radius to acoustic wavelength not negligible) goes back to Hasegawa [2], who used the near-field approach. This result was rederived with a far-field approach and elegantly expressed more recently by Mitri and Fellah [3].

The effect of viscosity on the mean force was considered by Westervelt [4]. However, his results were limited to $R \ll \lambda$ and $R \ll \delta$, in addition to the fact that the particle was fixed. Much later Doinikov [5] rigorously solved the first-order and second-order equations and came up with a mathematically involved equation for the force on a rigid spherical particle with no restrictions on the three length scales. He also extended this work to allow for compressible particles [6]. Moreover, Doinikov, in a series of papers [7–9], provided a general formula for the radiation force on particles in a viscous and heat conducting fluid. As pointed out by Settnes and Bruus [10], however, explicit analytical expressions were obtained only in the limits $\delta \ll R \ll \lambda$ and $R \ll \delta \ll \lambda$. Using the far-field approach, Settnes and Bruus [10] presented a general solution applicable for the limit $R,\delta \ll \lambda$, with no restriction on the relative thickness of the viscous layer compared to the particle size. Since their [10] work was primarily related to acoustophoreseis, considering $R/\lambda \ll 1$ proved to be sufficient. Further, they presented their arguments based on the scattering theory (time-retarded multipole expansion), where they expressed the scattered potential as a combination of monopole and dipole components. The viscous effects were built into the coefficients multiplying the dipole component.

In many situations of interest, $\delta \ll \lambda$, indicating that the viscous effect (decay) is generally small over a wavelength of the acoustic wave. Thus, even as the particle size increases and becomes comparable to the wavelength, the viscous effect on the incident wave itself is in general small and can be neglected. Only in special situations (for combinations of large fluid viscosity and very high frequency) all three length scales will be of comparable magnitude and both the finite-sized and viscous effects will be of importance. Therefore, in this work we assume that $\delta \ll \lambda$.

It is important to note that a portion of the incoming mean momentum flux is spent in generating acoustic streaming in the near field, while some part is scattered by the particle. As shown by Danilov and Mironov [11], integrating the stress tensor in the far field, one obtains the net second-order force acting on the particle. We will follow the far-field derivation approach in this work, therefore accounting for both the near-field streaming and the momentum flux carried by the sound waves, and thereby evaluate the net force on the particle.

*Corresponding author: bala1s@ufl.edu

The far-field approach has been used by Mitri [12] and Mitri and Fellah [3] to compute the radiation force on cylinders (plane traveling waves) and spheres (plane standing and quasistationary waves), respectively. The same authors in several papers (see [13,14]) have computed the radiation force using the near-field approach for spheres and cylinders and validated the same with those obtained using the far-field derivation.

The far-field approach naturally leads to an expansion, whose leading-order terms can be interpreted as contributions from interaction of monopole, dipole, and higher-order sources with the incident acoustic field and as contributions from mutual interactions between the monopole, dipole, and higher-order sources. Typical expressions of the mean force obtained in terms of such time-retarded multipole expansions have been limited to the dominant monopole and dipole contributions. The speed of convergence of the expansion or, more precisely, the adequacy of calculating the mean force based on only the monopole and dipole contributions can be expected to depend on the size of the particle relative to the wavelength of the acoustic field. Settnes and Bruus [10] alluded to this question of convergence and demonstrated the adequacy of their theoretical prediction based on monopole and dipole sources provided small particles were considered. Further, Bruus and co-workers studied the problem of acoustophoresis analytically [15] and verified their theory by conducting experiments [16,17]. Moreover, they used this theory in their numerical study of acoustopheric motion of microparticles [18,19]. Here, by obtaining a complete theoretical expansion for the mean force, we will examine the rate of convergence of the multipole expansion for both small- and finite-sized particles.

The purpose of the current work is as follows. We want to present a general solution that places limited restriction on the relative magnitude of the different length scales. The expression for the second-order time-averaged force obtained in the present study can be considered as an extension of the works by Hasegawa [2] and Mitri and Fellah [3] to a viscous compressible flow. Additionally, the force obtained can be interpreted in terms of a multipole expansion, similar to that of Settnes and Bruus [10], however to the case of a finite-sized particle, whose radius is not negligible compared to the wavelength.

In particular, we will show that monopole and dipole source terms are adequate to capture the mean force even in the case of finite-sized particles, provided $R/\lambda \lesssim 0.05$. However, in addition to the quadratic interaction of monopole and dipole sources with the incident sound field, we must also account for the quadratic interaction between the monopole and dipole sources. The higher-order terms (quadrupole, dipole-quadrupole cross terms, etc.) are shown to be important for particles sizes greater than 0.05λ. This idea of expressing the force in terms of monopole and dipole strengths has been eloquently presented in the works of Gor'kov [20] and Danilov and Mironov [11]. It may be noted that monopole-dipole cross terms was not included in [10], as the authors considered cases only where $R \ll \lambda$.

Finally, we recognize that the particle may be subjected to additional forces arising from external acoustic streaming. This streaming flow is due to the viscous effect associated with the emitter and reflector arrangement (external boundary conditions). Such forces are outside the scope of the present investigation since they depend on the specifics of the experimental setup.

II. PROBLEM FORMULATION

Here we consider a sphere in a viscous compressible but an otherwise stationary medium. In the presence of incident sound wave, the fluid is disturbed, whose motion will be described by the compressible Navier-Stokes equations

$$\frac{\partial \rho}{\partial t} + \nabla \cdot (\rho \mathbf{u}) = 0, \tag{1}$$

$$\rho\left(\frac{\partial \mathbf{u}}{\partial t} + \mathbf{u}\cdot\nabla\mathbf{u}\right) = -\nabla p + \mu\nabla^2\mathbf{u} + \left(\mu_b + \frac{1}{3}\mu\right)\nabla(\nabla\cdot\mathbf{u}). \tag{2}$$

The flow is assumed to be adiabatic and hence the pressure depends only on density as

$$p = p(\rho). \tag{3}$$

In the above equations, ρ is the fluid density, p is the pressure, $\mathbf{u}$ represents velocity, μ and μ_b denote the dynamic and bulk viscosities of the medium, respectively, and t represents time.

Before the acoustic wave is introduced into the medium, the fluid is assumed to be stationary and to possess constant properties. Once disturbed, the fluid properties can be expressed using perturbation theory as

$$\begin{aligned} \rho &= \rho_0 + \rho_1 + \rho_2 + \cdots, \\ p &= p_0 + p_1 + p_2 + \cdots, \\ \mathbf{u} &= \mathbf{u}_1 + \mathbf{u}_2 + \cdots, \end{aligned} \tag{4}$$

where the subscripts 0, 1, and 2 represent the base quantity and first-order and second-order perturbation quantities, respectively. The base quantities represent the undisturbed flow. The incoming sound wave creates the first-order disturbance. The reflected sound wave (due to the presence of the particle) is also first order in nature. However, the interaction between the incoming and scattered waves generates the second-order quantities, which are primarily responsible for the mean force under discussion. Quantitatively we define the perturbation quantities as

$$\begin{aligned} \frac{|\rho_i|}{\rho_0} &\propto \epsilon^i, \quad i = 0,1,2,\ldots \quad \text{for } \epsilon \ll 1, \\ \frac{|p_i|}{p_0} &\propto \epsilon^i, \quad i = 0,1,2,\ldots \quad \text{for } \epsilon \ll 1, \\ \frac{|\mathbf{u}_i|}{c_0} &\propto \epsilon^i, \quad i = 1,2,\ldots \quad \text{for } \epsilon \ll 1, \end{aligned}$$

where c_0 denotes the undisturbed ambient speed of sound and ϵ can be taken to be the ratio of the incoming sound wave velocity to the ambient speed of sound.

As defined before, we are interested in the time-averaged force. The incident sound wave is a first-order quantity that is harmonic in time. Consequently, averaging any time-harmonic quantity over one period would yield identically zero net force. However, second-order terms yield both second-harmonic and base-state modification; the latter will not vanish on time averaging and in fact contribute to the mean force. Therefore, the pursuit is to solve for the time-averaged second-order terms. It can be shown, however, that the mean second-order equations can be written solely in terms of the first-order quantities under certain limiting conditions, which will be discussed further. Towards this goal, we obtain the linearized Navier-Stokes equations.

Substituting Eq. (4) into Eqs. (1) and (2) yields

$$\frac{\partial \rho_1}{\partial t} + \rho_0 \nabla \cdot (\mathbf{u}_1) = 0 \tag{5}$$

and

$$\rho_0 \frac{\partial \mathbf{u}_1}{\partial t} = -\nabla p_1 + \mu \nabla^2 \mathbf{u}_1 + \left(\mu_b + \frac{1}{3}\mu\right)\nabla(\nabla \cdot \mathbf{u}_1). \tag{6}$$

Finally, the first-order pressure and density are related by the speed of sound c_0,

$$p_1 = c_0^2 \rho_1. \tag{7}$$

Now, since we are dealing with a viscous fluid, based on Helmholtz decomposition theorem, the first-order flow field can be written as a summation of an irrotational component and a rotational component

$$\langle w_1 \rangle = \langle w_{1A} \rangle + \langle w_{1V} \rangle, \tag{8}$$

where w_1 represents any first-order flow variable, the subscript A represents the irrotational (acoustic) part, and the subscript V stands for the rotational (vortical) part. By this definition, we have $\nabla \times \mathbf{u}_{1A} = 0$ and $\nabla \cdot \mathbf{u}_{1V} = 0$.

In a similar fashion, we now proceed to derive the second-order time-averaged equations. Again, substituting Eq. (4) in Eqs. (1) and (2) and collecting the second-order terms, followed by time averaging, gives

$$\rho_0 \nabla \cdot \langle \mathbf{u}_2 \rangle + \nabla \cdot \langle \rho_1 \mathbf{u}_1 \rangle = 0, \tag{9}$$

$$\left\langle \rho_1 \frac{\partial \mathbf{u}_1}{\partial t} \right\rangle + \rho_0 \langle \mathbf{u}_1 \cdot \nabla \mathbf{u}_1 \rangle = -\nabla \langle p_2 \rangle + \mu \nabla^2 \langle \mathbf{u}_2 \rangle + \left(\mu_b + \frac{1}{3}\mu\right)\nabla(\nabla \cdot \langle \mathbf{u}_2 \rangle), \tag{10}$$

where the angular brackets represent the quantity averaged over one time cycle, defined as

$$\langle g \rangle = \frac{1}{T}\int_0^T g(t)dt. \tag{11}$$

The second-order flow field can also be separated into acoustic and vortical components. However, making use of the linearity of the above equations, we write $\mathbf{u}_2 = \mathbf{u}_{2a} + \mathbf{u}_{2v}$ and $p_2 = p_{2a} + p_{2v}$. Using these definitions, in addition to Eq. (8) in Eqs. (9) and (10), and collecting terms involving the indices $1A$ and $2a$ we obtain

$$\rho_0 \nabla \cdot \langle \mathbf{u}_{2a} \rangle + \nabla \cdot \langle \rho_{1A} \mathbf{u}_{1A} \rangle = 0 \tag{12}$$

and

$$\left\langle \rho_{1A} \frac{\partial \mathbf{u}_{1A}}{\partial t} \right\rangle + \rho_0 \langle \mathbf{u}_{1A} \cdot \nabla \mathbf{u}_{1A} \rangle = -\nabla \langle p_{2a} \rangle + \mu \nabla^2 \langle \mathbf{u}_{2a} \rangle + \left(\mu_b + \frac{1}{3}\mu\right)\nabla(\nabla \cdot \langle \mathbf{u}_{2a} \rangle). \tag{13}$$

By subtracting Eqs. (12) and (13) from Eqs. (9) and (10), respectively, we obtain the corresponding equations for $\langle \mathbf{u}_{2v} \rangle$ and $\langle p_{2v} \rangle$. However, it must be noted that $\langle \mathbf{u}_{2a} \rangle$ and $\langle p_{2a} \rangle$ are not uniformly irrotational components of the second-order flow everywhere, meaning that $\nabla \times \mathbf{u}_{2a}$ will not be identically zero everywhere in the flow. As shall be described later, the mean force can be computed by integrating the momentum equation over a surface located in the inviscid bulk, provided it encloses the particle. Since, in the inviscid far field, the flow is a potential flow, we set $\mu = 0$ and $\mu_b = 0$ in Eq. (13). This leads to

$$\left\langle \rho_{1A} \frac{\partial \mathbf{u}_{1A}}{\partial t} \right\rangle + \rho_0 \langle \mathbf{u}_{1A} \cdot \nabla \mathbf{u}_{1A} \rangle = -\nabla \langle p_{2A} \rangle. \tag{14}$$

It is clear from Eqs. (12) and (14) that the mean second-order terms can be expressed purely in terms of the first-order quantities. Therefore, the next step is to solve for the first-order perturbations, which will be discussed in the forthcoming section. The set of equations for $\langle \mathbf{u}_{2v} \rangle$ involves the vortical terms and will account for acoustic streaming, which will not be explicitly dealt with in this work.

III. FIRST-ORDER EQUATIONS

Here we consider a plane sound wave propagating along the axial z direction with an angular frequency of ω in a viscous compressible medium incident on a finite-sized spherical particle. The velocity field thus generated can be written up to first order as

$$\mathbf{u}_1 = \nabla \phi + \nabla \times \Psi, \tag{15}$$

where ϕ represents the scalar velocity potential and Ψ is the vector velocity potential. Further, the scalar potential can be written as the sum of an incident potential ϕ_i and a scattered potential ϕ_{sc}. The plane incoming wave can be written in spherical coordinates as [21]

$$\phi_i = \sum_{n=0}^{\infty} C_n (2n+1) i^n j_n(kr) P_n(\cos\theta) e^{-i\omega t}, \tag{16}$$

where j_n represents spherical Bessel function of the first kind with order n, P_n denotes Legendre polynomials of the first kind with degree n, and C_n represents the complex amplitude of the wave and depends on the type of wave (traveling or standing). Here r and θ represent the radial and circumferential directions, respectively, with origin located at the particle center of mass, and the incoming wave has a wave number k given by

$$k = \frac{\omega}{c_0}\left[1 - \frac{i\omega}{\rho_0 c_0^2}\left(\mu_b + \frac{4}{3}\mu\right)\right]^{-1/2}. \tag{17}$$

Similarly, the scattered wave potential can be described as

$$\phi_{sc} = \sum_{n=0}^{\infty} C_n (2n+1) i^n S_n h_n(kr) P_n(\cos\theta) e^{-i\omega t}, \tag{18}$$

where h_n is the spherical Hankel function of the first kind with order n. Considering the fact that we are dealing with an axisymmetric problem, the vector potential Ψ can be reduced to a scalar potential ψ that satisfies

$$\nabla^2 \psi + k_v^2 \psi = 0, \tag{19}$$

where $k_v = (1+i)/\delta = \sqrt{i\omega/\nu}$, with ν and δ denoting the kinematic viscosity of the medium and the momentum boundary layer thickness, respectively. The solution of Eq. (19) yields

$$\psi = \sum_{n=0}^{\infty} C_n(2n+1)i^n S_{\nu n} h_n(k_\nu r) P_n(\cos\theta) e^{-i\omega t}. \quad (20)$$

In Eqs. (18) and (20), S_n and $S_{\nu n}$ are known as the scattering coefficients, which are to be evaluated based on the boundary conditions at the particle surface.

IV. EVALUATING THE PARTICLE VELOCITY IN TERMS OF SCATTERING COEFFICIENTS

To evaluate the first-order particle velocity, we begin with the expression of force. Since the flow is considered to be axisymmetric and the sphere is assumed to translate along the z axis, the hydrodynamic force acting on the particle (along the z direction) is given by

$$F_1 = 2\pi R^2 \int_0^{\pi} (\sigma_{rr}\cos\theta - \sigma_{r\theta}\sin\theta)|_{r=R} \sin\theta \, d\theta, \quad (21)$$

where the expressions for the stress tensor in terms of ϕ and ψ are given by [22]

$$\begin{aligned} \sigma_{rr} &= 2\mu\left[\left(\frac{1}{2\nu}\frac{\partial}{\partial t} - \nabla^2 + \frac{\partial^2}{\partial r^2}\right)\phi \right. \\ &\quad \left. + \left(r\frac{\partial^3}{\partial r^3} + 3\frac{\partial^2}{\partial r^2} - r\frac{\partial}{\partial r}\nabla^2 - \nabla^2\right)\psi\right], \\ \sigma_{r\theta} &= 2\mu\left[\left(\frac{\partial^2}{\partial r\partial\theta}\frac{1}{r}\right)\phi \right. \\ &\quad \left. + \left\{\frac{\partial}{\partial\theta}\left(\frac{\partial^2}{\partial r^2} + \frac{1}{r}\frac{\partial}{\partial r} - \frac{1}{r^2} - \frac{1}{2}\nabla^2\right)\right\}\psi\right]. \end{aligned} \quad (22)$$

The required spatial derivatives in Eq. (22) have been evaluated in Appendix A. Substituting Eqs. (A3)–(A10) and (19) in Eq. (21) gives

$$\begin{aligned} F_1 &= -4\pi\mu i (k_\nu R)^2 C_1[j_1(kR) + S_1 h_1(kR) \\ &\quad + 2S_{\nu 1} h_1(k_\nu R)] e^{-i\omega t}. \end{aligned} \quad (23)$$

It may be noted here that only the $n = 1$ term of ϕ and ψ survives the integration in Eq. (21). Now, representing the first-order particle velocity along the axial direction by u_p, the particle equation of motion is

$$F_1 = \rho_p V_p \frac{du_p}{dt}, \quad (24)$$

where ρ_p and V_p denote the particle density and volume, respectively. Equating Eqs. (23) and (24), and defining $\rho' = \rho_p/\rho_0$ one obtains an expression for particle velocity given by

$$u_p = \frac{3i}{\rho' R} C_1[j_1(kR) + S_1 h_1(kR) + 2S_{\nu 1} h_1(k_\nu R)] e^{-i\omega t}. \quad (25)$$

V. EVALUATING SCATTERING COEFFICIENTS

In this section, the scattering coefficients are obtained by equating the fluid velocity components at the particle surface to the particle velocity. The radial and circumferential velocity components of the ambient fluid in terms of the potentials are computed in Appendix A. Therefore, from Eqs. (A12) and (A13), the velocity components at $r = R$ are given by

$$\begin{aligned} u_r|_{r=R} &= \frac{1}{R}\sum_{n=0}^{\infty} C_n(2n+1)i^n\{[nj_n(kR) - kRj_{n+1}(kR)] \\ &\quad + S_n[nh_n(kR) - kRh_{n+1}(kR)] \\ &\quad + S_{\nu n}[n(n+1)h_n(k_\nu R)]\} P_n(\cos\theta) e^{-i\omega t}, \\ u_\theta|_{r=R} &= \frac{1}{R}\sum_{n=0}^{\infty} C_n(2n+1)i^n\{[j_n(kR)] + S_n[h_n(kR)] \\ &\quad + S_{\nu n}[(n+1)h_n(k_\nu R) - (k_\nu R)h_{n+1}(k_\nu R)]\} \\ &\quad \times \frac{\partial}{\partial\theta}[P_n(\cos\theta)] e^{-i\omega t}. \end{aligned} \quad (26)$$

Also, the fluid velocity at the surface of the particle in terms of u_p is given by

$$\begin{aligned} u_r|_{r=R} &= u_p\cos\theta = u_p P_1(\cos\theta), \\ u_\theta|_{r=R} &= -u_p\sin\theta = u_p\frac{\partial}{\partial\theta}[P_1(\cos\theta)], \end{aligned} \quad (27)$$

where the expression of u_p is as given in Eq. (25). For simplification purposes, we define the following:

$$\begin{aligned} nj_n(kR) - kRj_{n+1}(kR) &= f_{1n}, \quad j_n(kR) = g_{1n}, \\ nh_n(kR) - kRh_{n+1}(kR) &= f_{2n}, \quad h_n(kR) = g_{2n}, \\ n(n+1)h_n(k_\nu R) &= f_{3n}, \\ (n+1)h_n(k_\nu R) - (k_\nu R)h_{n+1}(k_\nu R) &= g_{3n}. \end{aligned}$$

Similar expressions have also been reported in the recent work by Guz [22]. However, it must be noted that the particle velocity expression (and, as a consequence, the first-order force formulation) provided in [22] has minor errors. With the above definitions, for $n \neq 1$, Eq. (26) when equated to Eq. (27) reduces to

$$\begin{aligned} f_{1n} + S_n f_{2n} + S_{\nu n} f_{3n} &= 0, \\ g_{1n} + S_n g_{2n} + S_{\nu n} g_{3n} &= 0. \end{aligned} \quad (28)$$

One can solve for the scattering coefficients (for $n \neq 1$) using Cramer's rule as

$$S_n = \frac{\begin{vmatrix} -f_{1n} & f_{3n} \\ -g_{1n} & g_{3n} \end{vmatrix}}{\begin{vmatrix} f_{2n} & f_{3n} \\ g_{2n} & g_{3n} \end{vmatrix}}, \quad S_{\nu n} = \frac{\begin{vmatrix} f_{2n} & -f_{1n} \\ g_{2n} & -g_{1n} \end{vmatrix}}{\begin{vmatrix} f_{2n} & f_{3n} \\ g_{2n} & g_{3n} \end{vmatrix}}. \quad (29)$$

A similar procedure for $n = 1$ gives

$$\begin{aligned} S_1 &= \frac{\begin{vmatrix} g_{11} - \rho' f_{11} & \rho' f_{31} - 2h_1(k_\nu R) \\ -(\rho'-1)g_{11} & \rho' g_{31} - 2h_1(k_\nu R) \end{vmatrix}}{\begin{vmatrix} \rho' f_{21} - g_{21} & \rho' f_{31} - 2h_1(k_\nu R) \\ (\rho'-1)g_{21} & \rho' g_{31} - 2h_1(k_\nu R) \end{vmatrix}}, \\ S_{\nu 1} &= \frac{\begin{vmatrix} \rho' f_{21} - g_{21} & g_{11} - \rho' f_{11} \\ (\rho'-1)g_{21} & -(\rho'-1)g_{11} \end{vmatrix}}{\begin{vmatrix} \rho' f_{21} - g_{21} & \rho' f_{31} - 2h_1(k_\nu R) \\ (\rho'-1)g_{21} & \rho' g_{31} - 2h_1(k_\nu R) \end{vmatrix}}. \end{aligned} \quad (30)$$

Now that the scattering coefficients (S_n, $S_{\nu n}$) have been computed, any first-order quantity can be completely described.

VI. SECOND-ORDER MEAN FORCE

The mean second-order force acting on a particle is given by

$$\langle \mathbf{F} \rangle = \left\langle \int_{S_0} \boldsymbol{\sigma} \cdot \mathbf{n}\, dS \right\rangle, \tag{31}$$

where $\boldsymbol{\sigma} = -p\boldsymbol{I} + \boldsymbol{\tau}$, with $\boldsymbol{I}$ and $\boldsymbol{\tau}$ representing the unit tensor and shear stress, respectively. Here $\mathbf{n}$ denotes the unit normal vector pointing away from the surface of the sphere S_0, which in itself varies periodically in time owing to particle oscillation about the mean position. It can be proven that

$$\langle \mathbf{F} \rangle = \left\langle \int_{S_0} \boldsymbol{\sigma} \cdot \mathbf{n}\, dS \right\rangle = \left\langle \int_{S_{ff}} (\boldsymbol{\sigma} - \rho_0 \mathbf{u} \otimes \mathbf{u}) \cdot \mathbf{n}\, dS \right\rangle, \tag{32}$$

where S_{ff} is any surface enclosing the particle (see [11,23,24]).

In ideal fluids, the mean force given by Eq. (32) is the same as the radiation force. However, in the case of viscous fluids, some mean momentum goes into generating a streaming flow near the particle surface. The reader is encouraged to refer to [11] for a detailed discussion on this subject. Therefore, in this work, using the far-field derivation approach, we compute the net force acting on the particle.

The advantages of this far-field-derivation approach include the following. First, the Hankel functions appearing in the velocity potentials reduce to exponentials as $r \to \infty$, thereby making the integrals easier to evaluate. Second, in the bulk, where viscous forces are negligible, the mean second-order terms can be expressed purely in terms of first-order quantities [see Eq. (14)]. Following [11], it can be shown that

$$\langle \mathbf{F}_2 \rangle = \int_{S_{ff}} \left[\frac{1}{2} \langle \mathbf{u}_{1A}^2 \rangle - \frac{1}{2\rho_0 c_0^2} \langle p_{1A}^2 \rangle - \rho_0 \langle \mathbf{u}_{1A} \cdot \mathbf{u}_{1A} \rangle \right] d\mathbf{S}_{ff}. \tag{33}$$

Therefore, Eq. (33) expresses the mean force only in terms of first-order quantities. Since we are integrating in the far field, only the acoustic part of flow properties survives, i.e., $\mathbf{u}_1 = \mathbf{u}_{1A}$ and $p_1 = p_{1A}$. Consequently, in the inviscid bulk, $\mathbf{u}_1 = \nabla \phi$ and $p_1 = -\rho_0 \frac{\partial \phi}{\partial t}$. As stated before, since we have already evaluated the scattering coefficients, the first-order pressure and velocity can now be computed. Consequently, the mean force can be expressed in terms of the scattering coefficients. It is important to note that, though we are integrating in the far field, the effects of viscosity are built into S_n and $S_{\nu n}$.

In most practical applications, the imaginary or decaying part of the wave number k [Eq. (17)] can be assumed to be negligible (i.e., $\omega\nu/c_0^2 \ll 1$). For example, in the field of acoustophoresis, where one deals with the passage of ultrasound waves ($\omega \sim 2\pi \times 1.5$ MHz), say, in human blood ($\rho_0 \sim 1050\ \mathrm{kg\,m^{-3}}$, $\nu \sim 10^{-6}\ \mathrm{m^2\,s^{-1}}$), the imaginary part of the wave number k will be of the order of 10^{-6}. Similarly, in pharmaceutical applications where levitation of particles in air is important, the frequencies used are in the range of 20–22 kHz, which also leads to negligible values of $\omega\nu/c_0^2$. Therefore, we may assume that $k \to k_0$, where k_0 represents the real part of the wave number k. Following along the lines of Mitri and Fellah [3], we make the following arguments. In the far field, as $k_0 r \to \infty$, the spherical Hankel function reduces to the exponential function

$$i^n h_n(k_0 r) \to \frac{e^{ik_0 r}}{ik_0 r}. \tag{34}$$

Therefore, based on the above simplification, the scattered velocity potential can be written as

$$\phi_{sc} = \frac{f(\theta) e^{ik_0 r}}{r} e^{-i\omega t}, \tag{35}$$

where

$$f(\theta) = \frac{1}{ik_0} \sum_{n=0}^{\infty} C_n (2n+1) S_n P_n(\cos\theta). \tag{36}$$

This new definition of the scattered potential in combination with the incident wave potential is substituted into Eq. (33) to obtain the time-averaged second-order force acting on a particle in the direction of the propagation of the wave. It is given by

$$\begin{aligned} \langle F_2 \rangle = & -\pi \rho_0 k_0^2 \int_0^\pi f(\theta) f^*(\theta) \sin\theta \cos\theta\, d\theta \\ & -\pi \rho_0 r^2 k_0^2 \int_0^\pi \mathrm{Re}\left(\tilde{\phi}_i^* \frac{f(\theta) e^{ik_0 r}}{r} \right) \sin\theta \cos\theta\, d\theta \\ & +\pi \rho_0 r^2 k_0^2 \int_0^\pi \mathrm{Im}\left(\frac{\partial \tilde{\phi}_i^*}{\partial z} \frac{f(\theta) e^{ik_0 r}}{r} \right) \sin\theta \cos\theta\, d\theta, \end{aligned} \tag{37}$$

where $\tilde{\phi}_i = \phi_i e^{i\omega t}$, the asterisk represents the complex conjugate, and Re and Im denote the real and imaginary parts, respectively.

A. Standing wave

In this section, we compute the force on a particle in the presence of a standing wave. For the case of a standing wave, $C_n = \phi_0 [e^{ik_0 h} + (-1)^n e^{-ik_0 h}]$, where ϕ_0 is the amplitude of the incoming wave and h is the distance between the particle center of mass and the nearest pressure antinode. Hasegawa and Yosioka in a series of papers [2,25–27] expressed this force as a nondimensional quantity, the so-called radiation force function, given by

$$Y_{st}^{ff} = \frac{\langle F_2 \rangle_{st}}{\sin(2k_0 h) \langle E \rangle A}, \tag{38}$$

where $\langle E \rangle = \frac{1}{2} \rho_0 \phi_0^2 k_0^2$ is the time-averaged incident energy density and $A = \pi R^2$ is the cross-sectional area of the sphere. The indices st and ff denote that this force has been obtained for a standing wave and using the far-field approach, respectively. Now substituting Eqs. (16) and (36) in Eq. (37) and defining $S_n = \alpha_n + i\beta_n$ we obtain

$$\begin{aligned} Y_{st}^{ff} = \sum_{n=0}^{\infty} \frac{8}{(k_0 R)^2} (-1)^{n+1} [(2n+1)\beta_n \\ - 2n(\alpha_n \beta_{n-1} - \alpha_{n-1} \beta_n)]. \end{aligned} \tag{39}$$

In the inviscid limit, Mitri and Fellah [3] obtained an expression for the radiation force function given by

$$\left(Y_{st}^{ff}\right)_{MF} = \sum_{n=0}^{\infty} \frac{8}{(k_0R)^2}(-1)^{n+1}[\beta_n + 2(n+1) \times (\alpha_{n+1}\beta_n - (1+\alpha_n)\beta_{n+1})], \quad (40)$$

where the subscript MF denotes that this expression [Eq. (40)] was obtained by Mitri and Fellah [3]. It may be observed that on expanding the series both Eqs. (39) and (40) lead to the same expression. However, it must be noted that the expression in Eq. (39) has been derived for a viscous problem and as a result the α and β incorporate the viscous effects in them. The terms in our expression for the force given by Eq. (39) have been arranged to better correspond to a multipole expansion, similar to that given by Settnes and Bruus [10].

For example, in Eq. (39), $n = 0$ corresponds to the monopole term, $n = 1$ corresponds to dipole and monopole-dipole quadratic terms, and so on. In the case of a standing wave, the $n = 0$ term of Eq. (39) yields

$$\left(Y_{st}^{ff}\right)_1 = \left(Y_{st}^{ff}\right)_M = -\frac{8\beta_0}{(k_0R)^2}, \quad (41)$$

where the index 1 denotes that this term arises from the first term of Eq. (39) and the subscript M denotes the monopole. In the above expression, β_0 is defined as the monopole strength. Qualitatively, this is equivalent to the ejection of mass from the source (sphere) due to scattering of the incident sound wave by the particle. Ideally, in the absence of a particle, there would be no scattering of the incoming wave. However, in the presence of a particle, the incoming wave is scattered and can be thought of as the ejection of the incoming mass of fluid. Quantitatively, the leading-order scattered potential in Eq. (18) becomes independent of the polar coordinate θ [since $P_0(\cos\theta) = 1$] and depends only on the radial coordinate r. Further, the functional dependence of the radial coordinate is a zeroth order spherical Hankel function of the first kind, which is reminiscent of an outgoing spherical wave.

While the monopole can be considered to be a mass source, the dipole is a momentum source. There is no net mass outflow, but only momentum exchange, which will lead to a net force in the direction of particle oscillation. The $n = 1$ term in Eq. (39) yields

$$\left(Y_{st}^{ff}\right)_2 = \left(Y_{st}^{ff}\right)_D + \left(Y_{st}^{ff}\right)_{MD} = \frac{8}{(k_0R)^2}[3\beta_1] + \frac{8}{(k_0R)^2}[2(\alpha_0\beta_1 - \alpha_1\beta_0)], \quad (42)$$

where $(Y_{st}^{ff})_D$ is the contribution only due to the dipole and $(Y_{st}^{ff})_{MD}$ is the monopole-dipole contribution. Similarly, higher-order terms can be given a physical interpretation. As can be seen from the expression of $(Y_{st}^{ff})_D$, only the imaginary part of S_1, i.e., β_1, contributes. As mentioned earlier, since the dipole is related to the first-order force, it is worthwhile to refer to Eq. (23). This first-order force expression involves three terms. While the first term $j_1(kR)$ arises due to the incoming wave, the second term $S_1h_1(kR)$ is due to the scattered potential and contributes to the dipole strength β_1. The third term $S_{v1}h_1(k_vR)$ does not enter the dipole expression as we are integrating in the far field and consequently this term decays as $r \to \infty$. Finally, it must be noted that while the monopole and dipole strengths involve only the imaginary part of the scattering coefficients, the monopole-dipole cross term $(Y_{st}^{ff})_{MD}$, which is the quadratic interaction between the monopole and dipole, involves the cross talk between the real part of the monopole with the imaginary part of the dipole and vice versa. Before assessing the effect of the various terms on the mean force, we make the following observation. Settnes and Bruus [10] also expressed the radiation force (in a viscous compressible medium) in terms of monopole and dipole strengths, in the small-particle-size (relative to acoustic wavelength) limit. They observed that in the case of a standing wave, only the real parts of the monopole and dipole sources contributed to the mean force and their expressions for these contributions can be expressed as

$$\left(Y_{st}^{ff}\right)_{M,SB} = \frac{8}{3}(k_0R)\mathrm{Re}\left(1 - \frac{1}{\rho'}\frac{c_0^2}{c_p^2}\right),$$

$$\left(Y_{st}^{ff}\right)_{D,SB} = 4(k_0R)\mathrm{Re}\left[\frac{2(\rho'-1)\left\{1 + \frac{3}{2}\frac{\delta}{R}\left(1 + i + i\frac{\delta}{R}\right)\right\}}{2\rho' + 1 + \frac{9}{2}\frac{\delta}{R}\left(1 + i + i\frac{\delta}{R}\right)}\right], \quad (43)$$

where the subscript SB represents the expressions provided by Settnes and Bruus [10] and c_p is the speed of sound inside the particle. In the limit of $R \ll \lambda$, the generic expressions for the monopole $(Y_{st}^{ff})_M$ and dipole $(Y_{st}^{ff})_D$ reduce to Eq. (43). This can be seen in Fig. 1, where we compare the generic expression for the dipole $(Y_{st}^{ff})_D$ with the limiting case $(Y_{st}^{ff})_{D,SB}$. Clearly, the results are identical for $R \ll \lambda$ and the deviation can be observed as R/λ increases, where the exact value of

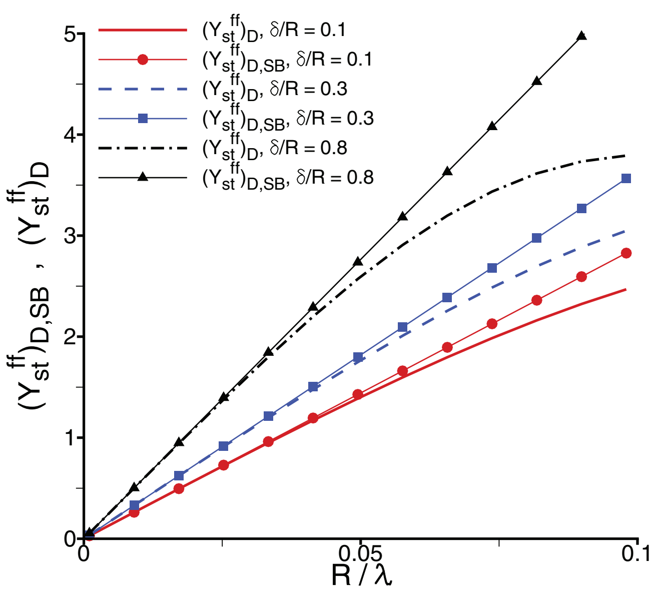

FIG. 1. (Color online) Dipole contribution from the current work $(Y_{st}^{ff})_D$ compared against that for the limiting case of $R \ll \lambda$ given by $(Y_{st}^{ff})_{D,SB}$ for a standing wave with varying δ/R. The results plotted with a solid line with circles, squares, and triangles, respective, are taken from Ref. [10] [see Eq. (43)]. The results are shown for $\rho' = 1000$ and $\mu_b/\mu = 0$.

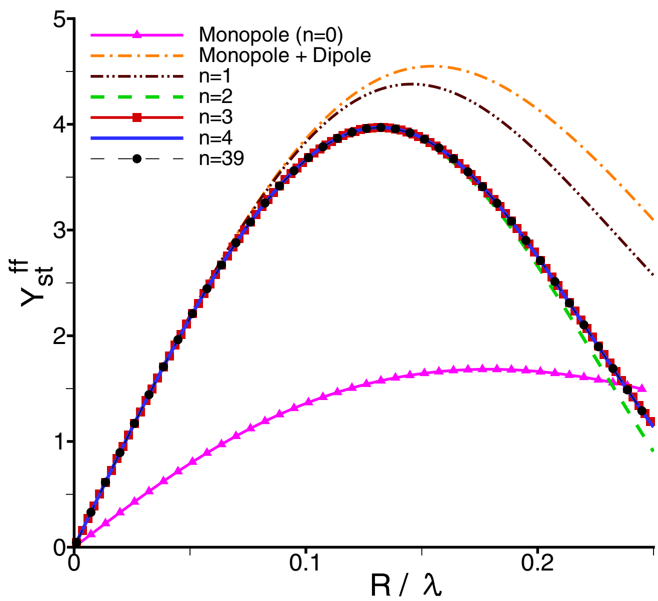

FIG. 2. (Color online) Effect of including progressively-higher-order terms (rate of convergence) on the radiation force function for a standing wave. The results are shown for $\rho' = 1000$, $\mu_b/\mu = 0$, and $\delta/R = 0.1$.

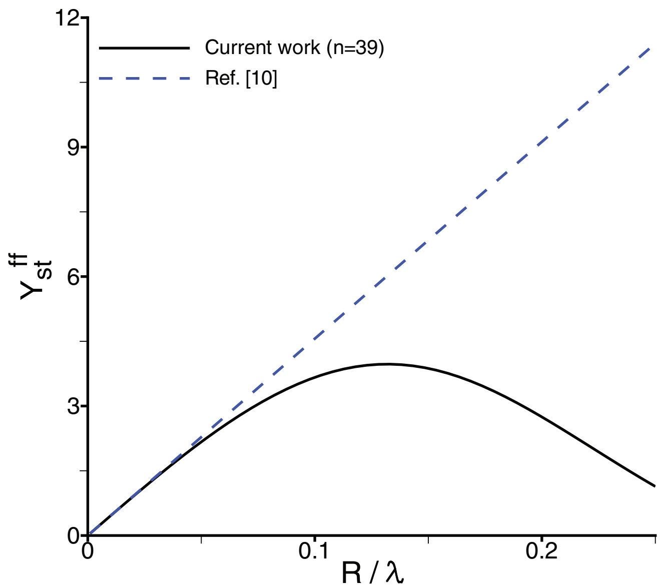

FIG. 3. (Color online) Radiation force function for finite-sized particles in a standing acoustic wave using the current formulation (solid line) [Eq. (39)], with $n = 39$, in comparison with the work of [10] (dashed line) (applicable for low R/λ). The results are shown for $\rho' = 1000$, $\mu_b/\mu = 0$, and $\delta/R = 0.1$.

this deviation depends on δ/R. As far as the monopole is concerned, it can be analytically shown (see Appendix B) that $(Y_{st}^{ff})_M$ reduces to $(Y_{st}^{ff})_{M,SB}$ in the small-particle-size limit. Therefore, for particles of size comparable to the acoustic wavelength, the general expressions provide a more accurate estimation of the monopole and dipole contributions.

Figure 2 shows the effect of including progressively-higher-order terms in computing the acoustic radiation force function. In this particular case, we compute the mean force on a nearly fixed rigid particle (achieved by letting the density ratio ρ' be 1000) in a medium whose bulk viscosity is zero. Further, the effect of kinematic viscosity has been incorporated by setting the momentum diffusion thickness δ to be 10% of the particle radius ($\delta/R = 0.1$). The range of R/λ has been chosen such that the imposed limitation $\delta \ll \lambda$ holds true. This analysis will shed light on the rate of convergence (number of terms required to accurately compute the mean force) that was mentioned in Sec. I. Clearly, Fig. 2 suggests that the monopole is insufficient to capture the force even for small values of R/λ. The hypothesis by Settnes and Bruus [10], that the force be represented in terms of monopole and dipole source strengths for small values of R/λ, is tested by just choosing $(Y_{st}^{ff})_M$ arising due to $n = 0$ and the $(Y_{st}^{ff})_D$ contribution arising from $n = 1$ in Eq. (39). As can be observed from the figure, for particles much smaller than the wavelength (for $R/\lambda \leqslant 0.05$), the monopole and dipole terms prove sufficient to capture the mean force. It must be noted here that, though we have included only the monopole and dipole strengths, the definitions given in Eqs. (41) and (42) include the effect of particle size. That is the reason we observe the radiation force function to decay after reaching a maximum at $R/\lambda \sim 0.15$. Instead, if the expressions provided in Eq. (43) are used [10], one would observe a continuous increase in the second-order mean force with increasing particle size. This behavior is shown in Fig. 3, which compares the current work with that of [10]. Here, in Fig. 3, it is clear that even for a particle of radius 5% (or more) of the acoustic wavelength, one needs to use the present finite-particle-size formulation. Moreover, the current formulation captures the maximum force that can be exerted on a particle in a plane standing wave and predicts that the mean force on a particle cannot monotonically increase with particle radius. Now, in reference to Fig. 2, the addition of the monopole-dipole cross term $(Y_{st}^{ff})_{MD}$ arising from $n = 1$ in Eq. (39) does contribute in better predicting the mean force for relatively larger particles. This monopole-dipole cross term does aid in reducing the maximum force as well as the value of R/λ at which the maximum force can be realized. Proceeding similarly, by including higher-order terms, we have observed that four terms ($n = 3$) are sufficient to accurately compute the mean force on the particle. This can also be seen in Fig. 2, where the difference in radiation force function between the $n = 3$ and 39 curves is negligible for $R/\lambda \leqslant 0.25$. For even larger particles, the first four terms ($n = 3$) of the multipole expansion will not be sufficient and the error will increase with increasing R/λ. In general, truncation at any finite value of n will be adequate only for a range of R/λ below a critical value. Henceforth, all results presented involving the current formulation will include the first 40 terms ($n = 39$) for $R/\lambda \leqslant 0.25$. In summary, for an extremely-small-sized particle one could use just the monopole and dipole strengths to evaluate the mean force, whereas, for finite-sized particles, one needs to use the current formulation [Eq. (39)] by including higher-order terms. Table I represents the value of R/λ up to which a given number of terms [in Eq. (39)] is sufficient to capture the mean force within 1% error. For this purpose, we have assumed that the solution (mean force) obtained using

TABLE I. Value of R/λ up to which the mean force on a particle in a standing wave can be accurately computed (within 1% error) with a given number of terms [in Eq. (39)]. The error is calculated based on the mean force computed using the first 40 terms.

Number of terms	n	R/λ
monopole (M) only (1)	0	0.0
M + dipole (D)		0.0235
Ref. [10]		0.0485
M + D + MD cross terms (2)	1	0.0498
3	2	0.1662
4	3	0.2462
5	4	0.2963

the first 40 terms ($n = 39$) accurately represents the force, meaning that the series in Eq. (39) has converged. Again, the numbers in the table have been obtained for a particle to fluid density ratio of 1000, $\delta/R = 0.1$, and zero bulk viscosity.

1. Comparison with numerical (computational fluid dynamics) results

In the inviscid limit, as described before, there exists extensive theoretical work in the literature [2,3,12–14,26,27] to calculate the mean force (acoustic radiation force) on finite-sized particles. In this work we have provided a closed-form analytical expression for the mean force in situations where both viscosity is important and the finite particle size cannot be ignored in comparison to the acoustic wavelength. Relative to the inviscid regime, the amount of experimental or numerical work in the viscous finite-particle-size regime is limited. A finite-element analysis (FEA) approach to evaluate the mean force in the regime of present interest was recently reported by Foresti *et al.* [28]. In order to validate our results, we compared our current theoretical formulation with the computational fluid dynamics (CFD) studies of [28]. The authors studied the stability of the spherical particles in the standing acoustic wave field in addition to the mean force on those particles. For this purpose, they used an axisymmetric levitator (see [28] and references therein), with the height fixed between the emitter and reflector. Figure 4 presents a comparison of the force computed in their FEA approach with the analytical prediction of Eq. (39) using $n = 39$ for varying R/λ. It can be observed from Fig. 4 that the second-order mean force increases (for both inviscid and viscous cases) up to a given value of R/λ and then decreases. However, the peak force achieved using the FEA analysis is off by about 12% (for the inviscid case) that achieved using the current theoretical formulation. Further, the value of R/λ at which this peak force is realized is offset by about 17.5%. In the inviscid limit, their numerical (FEA) results deviated from the theoretical results of Hasegawa *et al.* [29] for finite-size particles. They attributed this deviation to the dependence of the mean force on the three dimensionality of the actual emitter-reflector dimensions. Our expression [Eq. (39)] reduces to the correct inviscid behavior given by Mitri and Fellah [3] and Hasegawa [2]. Therefore, we believe that, in the inviscid limit, the difference between our work and that of the FEA [28] can be attributed to the source and/or reflector details chosen by Foresti *et al.* [28] and departure from the perfectly planar incident wave configuration. Given the margin of error discussed above, we observe that the comparison between the CFD results and our formulation are reasonable. In the viscous computations, for a standing wave, they computed the mean force for two different fluid viscosities: (i) viscosity of air ($\mu/\rho_0 = 1.55 \times 10^{-5}$ m^2 s^{-1}) and (ii) 100 times the viscosity of air ($\mu/\rho_0 = 1.55 \times 10^{-3}$ m^2 s^{-1}). Again, similar to that in the inviscid limit, the comparison is qualitatively very reasonable even in the viscous regime. The choice of viscosities made in [28] does not show substantial deviation from the inviscid case. Consequently, we considered a higher viscosity (1000 times the viscosity of air) and computed the mean force using the present formulation [Eq. (39)]. The results are shown in Fig. 4, where we clearly observe a significant decrease (8%) in the mean force compared to the inviscid case.

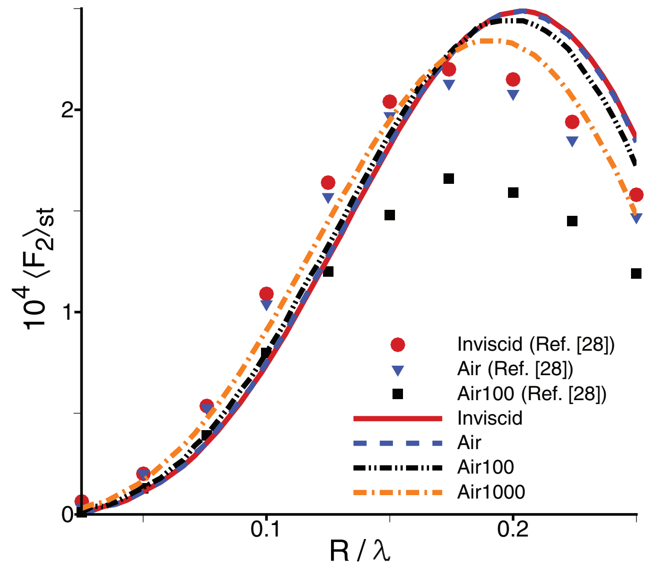

FIG. 4. (Color online) Comparison of the dimensional second-order mean force on a spherical particle in a standing wave [Eq. (39) using $n = 39$], represented by lines with the finite-element results of Foresti *et al.* [28], represented by symbols. The results are shown for $\rho' = 1000$ and $\mu_b/\mu = 0$ for three cases as discussed in [28]: inviscid ($\mu/\rho_0 = 0$, circles and solid line), viscosity of air ($\mu/\rho_0 = 1.55 \times 10^{-5}$ m^2 s^{-1}, triangles and dashed line), and 100 times the viscosity of air ($\mu/\rho_0 = 1.55 \times 10^{-3}$ m^2 s^{-1}, squares and dash–double-dotted line). Also shown is the mean force computed for 1000 times the viscosity of air ($\mu/\rho_0 = 1.55 \times 10^{-2}$ m^2 s^{-1}, dash-dotted line) using the present formulation.

2. Effect of kinematic viscosity on the mean force

The effect of kinematic viscosity on the mean force on a particle located in the midst of a standing wave is shown in Fig. 5. All results presented are for a density ratio of 1000 and $\mu_b/\mu = 0$. For extremely small particles $R/\lambda \ll 1$, the increase in viscosity only marginally increases the radiation force function. Settnes and Bruus [10] also observed a minor increase in the radiation force on a particle in a standing wave with increasing viscosity. Here the increase in mean force on the particle can be as large as 16% (for the case of $\delta/R = 0.2$ compared to the inviscid case). However, the difference in

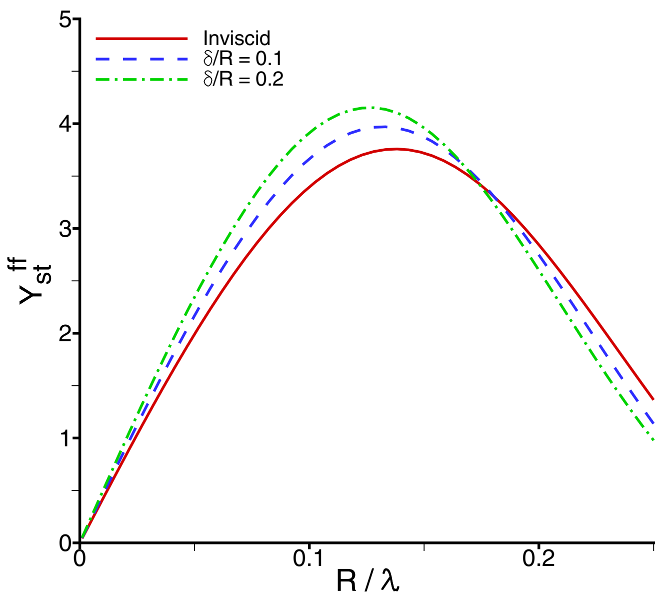

FIG. 5. (Color online) Effect of viscosity on the radiation force function [Eq. (39) with the first 40 terms] for a particle located in a standing-wave field. The results are shown for $\rho' = 1000$ and $\mu_b/\mu = 0$.

magnitude between the viscous and inviscid cases gradually rises, reaching a maximum at R/λ of approximately 0.125. Any further increase in R/λ leads to a decrease in the mean force with increasing viscosity. This reverse trend is consistent with the recent observations made in [28].

3. Effect of particle to fluid density ratio and bulk viscosity

Here we present the results due to a varying particle to fluid density ratio in addition to the effect of bulk viscosity on the mean force. As can be seen from Fig. 6, increasing

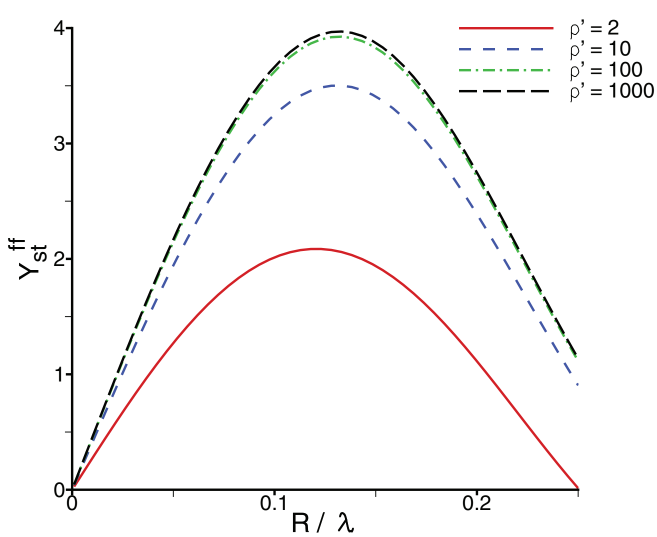

FIG. 6. (Color online) Effect of the density ratio ($\rho' = \rho_p/\rho_0$) on the radiation force function [Eq. (39) with the first 40 terms] for a particle located in a standing-wave field. The results are shown for $\delta/R = 0.1$ and $\mu_b/\mu = 0$.

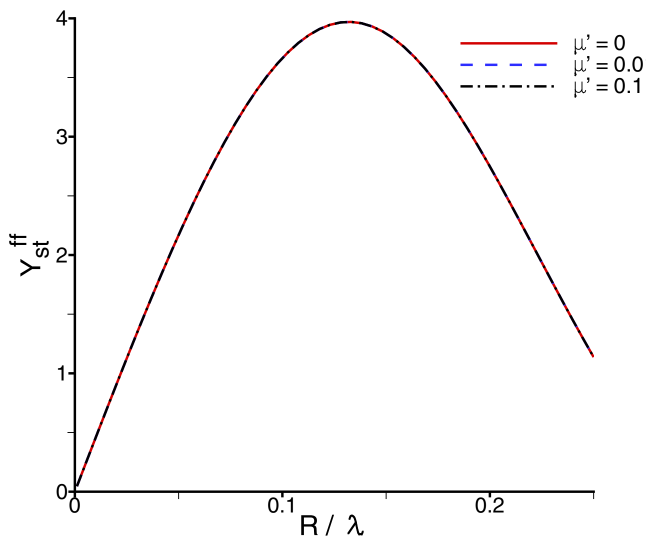

FIG. 7. (Color online) Effect of the bulk viscosity on the radiation force function [Eq. (39) with the first 40 terms] for a particle located in a standing-wave field. The results are shown for $\rho' = 1000$ and $\delta/R = 0.1$. Here $\mu' = \mu_b/\mu$.

the density ratio does increase the radiation force function. On reaching a density ratio of 100, the mean force tends to saturate, representing the behavior of a fixed rigid particle. Finally, we observe from Fig. 7 that the bulk viscosity has no effect on the force function.

B. Traveling wave

Following an approach similar to that in Sec. VI A but with $C_n = \phi_0$ in Eq. (16), we can represent a traveling wave from which we obtain the mean force due to a traveling wave. This force is expressed in nondimensional form as

$$Y_{tr}^{ff} = \frac{\langle F_2 \rangle_{tr}}{\langle E \rangle A}, \quad (44)$$

where the subscript tr denotes traveling wave. The radiation force function thus obtained is given by

$$Y_{tr}^{ff} = \sum_{n=0}^{\infty} -\frac{4}{(k_0 R)^2}[(2n+1)\alpha_n + 2n(\alpha_n \alpha_{n-1} + \beta_n \beta_{n-1})]. \quad (45)$$

Again, the viscous effects are built into the real and imaginary parts of the scattering coefficients (α and β). Further, this expression reduces to that provided by Hasegawa [27] in the inviscid limit.

Similar to the analysis performed in the previous section (on a standing wave), we study the rate of convergence in computing the mean force for finite-sized particles in a traveling wave. Figure 8 shows the effect of the number of terms [Eq. (45)] required to compute the mean force due to a traveling wave. As before, $\rho' = 1000$, $\mu_b/\mu = 0$, and $\delta/R = 0.1$. With these parameters, we present in Table II the value of R/λ up to which a given number of terms is sufficient to capture the mean force (on a particle situated in a traveling-wave field) within 1% error (assuming solution

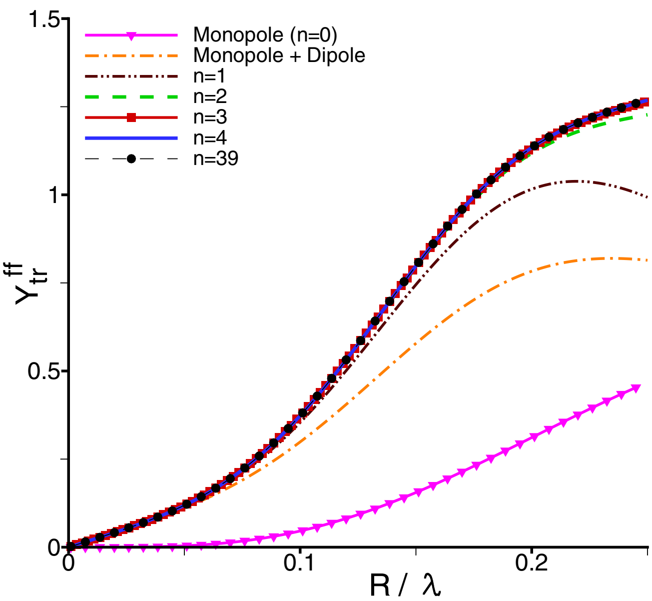

FIG. 8. (Color online) Effect of including progressively-higher-order terms (rate of convergence) on the radiation force function for a traveling wave. The results are shown for $\rho' = 1000$, $\mu_b/\mu = 0$, and $\delta/R = 0.1$.

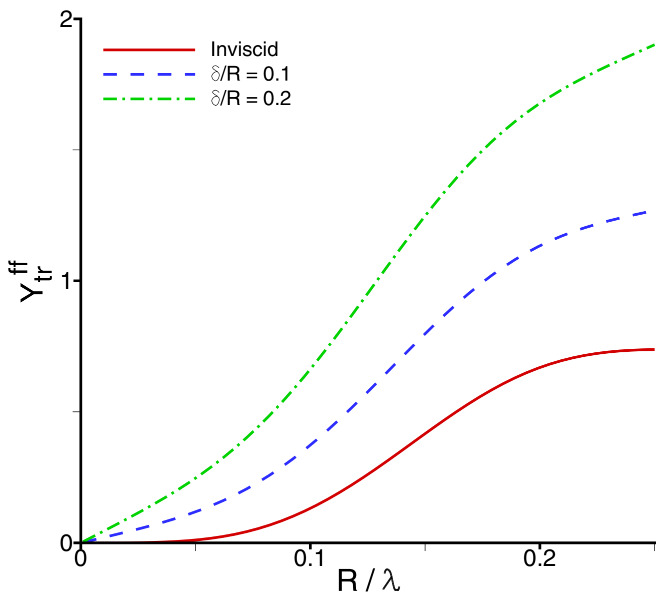

FIG. 9. (Color online) Effect of viscosity on the radiation force function [Eq. (45) with the first 40 terms] for a particle located in a traveling-wave field. The results are shown for $\rho' = 1000$ and $\mu_b/\mu = 0$.

converges with 40 terms). Here again we observe that a minimum of four terms is required to accurately evaluate the force for $R/\lambda \leqslant 0.25$. For even larger particles, additional terms in Eq. (45) will be required for accurate evaluation of the mean force. The interesting point is that, unlike the standing wave where the addition of the monopole-dipole quadratic term did not significantly modify the solution estimate, the cross term substantially improves the mean force computation. The effect of viscosity can be seen in Fig. 9, where the radiation force function is plotted as a function of R/λ. Here we observe that the effect of viscosity is significant. Danilov and Mironov [11] and Settnes and Bruus [10] also reported an increase in the mean force with viscosity for small-sized particles. Settnes and Bruus [10] reported an increase in the radiation force by a factor of $(2\pi R/\lambda)^{-3}$. This behavior was attributed to the interference between the incident and scattered waves that survives in the presence of viscosity (absent in the inviscid case) [10,11]. Here we observe that the viscous effects are dominant even for finite particle sizes. As can be seen from Fig. 9, the mean force increases by factors of 1.7 and 2.5 for $\delta/R = 0.1$ and 0.2 (at $R/\lambda = 0.25$), respectively, compared to the inviscid theory. In fact, in terms of an increase in the value of Y_{tr}^{ff}, the viscous effects can be seen to increase with R/λ. Finally, the mean force increases with increasing particle to fluid density ratio and remains unaffected by changes in bulk viscosity (figures not shown). This behavior is identical to that observed for a standing wave (Sec. VI A).

TABLE II. Value of R/λ up to which the mean force on a particle in a traveling wave can be accurately computed (within 1% error) with a given number of terms [in Eq. (45)]. The error is calculated based on the mean force computed using the first 40 terms.

Number of terms	n	R/λ
monopole (M) only (1)	0	0.0
M + dipole (D)		0.0185
Ref. [10]		0.0235
M + D + MD cross terms (2)	1	0.0323
3	2	0.1824
4	3	0.3065
5	4	0.4389

VII. CONCLUSION

The mean force on a finite-sized particle in a viscous compressible medium was considered and an analytical expression to compute the same was provided. Three length scales were involved in our analysis: the wavelength λ of the sound wave, the particle radius R, and the momentum-diffusion thickness δ. While δ/R and R/λ were arbitrary, the boundary-layer thickness was assumed to be much smaller compared to the wavelength. A far-field derivation approach was incorporated in determining the force due to plane standing and traveling waves. The flow properties were expanded up to second-order terms using perturbation theory and the force was expressed as a sum of infinite series. Based on the scattering theory, this infinite series could be physically interpreted as a multipole expansion, where the $n = 0$ term represented the monopole, $n = 1$ yielded the dipole and monopole-dipole quadratic term, and so on. Further, it was observed that the radiation force could be reasonably approximated using just the monopole, dipole, and their cross terms for $R/\lambda \lesssim 0.05$ for standing waves, while in the case of traveling waves, the limit was $R/\lambda \lesssim 0.03$. The analytical result for the mean force obtained in the present work is valid for finite-sized particles of arbitrary radius compared to the acoustic wavelength (the only limitation is that the viscous length is smaller than the wavelength). However, in plotting the results we have limited our attention to $R/\lambda \leqslant 0.25$. Thus we can consider large values of δ/R and not violate the requirement $\delta/\lambda \ll 1$. We observe that for $R/\lambda \leqslant 0.25$, even four terms ($n = 3$) are sufficient to provide a very accurate estimation of the mean force.

Both the standing- and traveling-wave solutions correctly reduced to their corresponding inviscid limits provided by Mitri and Fellah [3] and Hasegawa [2,27]. Further, for extremely small particle sizes, in the viscous regime, we found our results to be identical to that provided by Settnes and Bruus [10]. Moreover, we expressed our monopole and dipole strengths in terms of the monopole and dipole strengths of [10]. We noted that experimental and numerical data for finite-sized particles in the viscous limit are extremely limited. Consequently, in our regime of interest ($0 \leqslant R/\lambda \leqslant 0.25$), we compared our results (standing wave) with the recent FEA results of Foresti *et al.* [28]. The comparison was found to be reasonable. We argued that any differences between the CFD studies and our current formulation could be related to the emitter and/or reflector dimensions used in [28]. The kinematic viscosity substantially increased the mean force in the case of a traveling wave while having a relatively minimal effect on particles situated in a standing-wave field. We observed that for both traveling and standing waves, increasing the density ratio led to an increase in the mean force while remaining unchanged to variations in bulk viscosity. Additionally, the results presented for the viscous case assumed that $\omega\nu/c_0^2 \ll 1$. Finally, it must be noted that the current work neglects any effects due to the so-called external acoustic streaming.

ACKNOWLEDGMENTS

This work benefited from the US Department of Energy, National Nuclear Security Administration, Advanced Simulation and Computing Program, as a Cooperative Agreement under the Predictive Science Academic Alliance Program, under Contract No. DE-NA0002378.

APPENDIX A: RECURRENCE RELATIONS AND SPATIAL DERIVATIVES OF VELOCITY POTENTIALS

To compute the stresses and velocities, we need to evaluate the time and space derivatives of $\phi = \phi_i + \phi_{sc}$ and ψ. Thus, as a first step we derive these expressions in this section. To achieve this we will require the so-called recurrence relations. These relations express the spherical Bessel and Hankel derivatives in terms of their corresponding function values.

In the following equations (A1) and (A2), z is a complex number, f_n could represent either j_n or h_n, and the prime denotes differentiation with respect to z:

$$f_n'(z) = f_{n-1}(z) - \frac{n+1}{z} f_n(z), \quad n = 1,2,\ldots, \tag{A1}$$

$$f_n'(z) = -f_{n+1}(z) + \frac{n}{z} f_n(z), \quad n = 0,1,2,\ldots. \tag{A2}$$

Before proceeding with computing the spatial derivatives, it is important to note that the scalar potential satisfies the Helmholtz equation

$$\nabla^2\phi + k^2\phi = 0. \tag{A3}$$

From the definition of ϕ_i and using Eq. (A2),

$$\begin{aligned}\frac{\partial \phi_i}{\partial r} &= \sum_{n=0}^{\infty} C_n(2n+1)i^n\left\{-kj_{n+1}(kr) + \frac{n}{r}j_n(kr)\right\}P_n(\cos\theta)e^{-i\omega t}\\ &= \frac{1}{r}\sum_{n=0}^{\infty} C_n(2n+1)i^n\{nj_n(kr) - (kr)j_{n+1}(kr)\}P_n(\cos\theta)e^{-i\omega t}.\end{aligned} \tag{A4}$$

Differentiating Eq. (A4) and using Eq. (A1),

$$\begin{aligned}\frac{\partial^2 \phi_i}{\partial r^2} &= \sum_{n=0}^{\infty} C_n(2n+1)i^n\left[-k\left\{kj_n(kr) - \frac{n+2}{r}j_{n+1}(kr)\right\} - \frac{n}{r^2}j_n(kr)\right.\\ &\quad\left. + \frac{n}{r}\left\{-kj_{n+1}(kr) + \frac{n}{r}j_n(kr)\right\}\right]P_n(\cos\theta)e^{-i\omega t}\\ &= \frac{1}{r^2}\sum_{n=0}^{\infty} C_n(2n+1)i^n[(n^2-n)j_n(kr) - r^2k^2j_n(kr) + 2(kr)j_{n+1}(kr)]P_n(\cos\theta)e^{-i\omega t}.\end{aligned} \tag{A5}$$

Similarly,

$$\frac{\partial \phi_{sc}}{\partial r} = \frac{1}{r}\sum_{n=0}^{\infty} C_n(2n+1)i^n S_n\{nh_n(kr) - (kr)h_{n+1}(kr)\}P_n(\cos\theta)e^{-i\omega t}, \tag{A6}$$

$$\frac{\partial^2 \phi_{sc}}{\partial r^2} = \frac{1}{r^2}\sum_{n=0}^{\infty} C_n(2n+1)i^n S_n[(n^2-n)h_n(kr) - r^2k^2h_n(kr) + 2(kr)h_{n+1}(kr)]P_n(\cos\theta)e^{-i\omega t}, \tag{A7}$$

$$\frac{\partial \psi}{\partial r} = \frac{1}{r}\sum_{n=0}^{\infty} C_n(2n+1)i^n S_{vn}\{nh_n(k_v r) - (k_v r)h_{n+1}(k_v r)\}P_n(\cos\theta)e^{-i\omega t}, \tag{A8}$$

$$\frac{\partial^2\psi}{\partial r^2} = \frac{1}{r^2}\sum_{n=0}^{\infty} C_n(2n+1)i^n S_{\nu n}\big[(n^2-n)h_n(k_\nu r) - r^2k_\nu^2 h_n(k_\nu r) + 2(k_\nu r)h_{n+1}(k_\nu r)\big]P_n(\cos\theta)e^{-i\omega t}. \quad \text{(A9)}$$

Finally, differentiating Eq. (A9) with respect to r and using Eqs. (A1) and (A2),

$$\begin{aligned}\frac{\partial^3\psi}{\partial r^3} &= \frac{1}{r^2}\sum_{n=0}^{\infty} C_n(2n+1)i^n S_{\nu n}\bigg[(n^2-n)\bigg\{-k_\nu h_{n+1}(k_\nu r) + \frac{n}{r}h_n(k_\nu r)\bigg\}\\ &\quad - r^2k_\nu^2\bigg\{-k_\nu h_{n+1}(k_\nu r) + \frac{n}{r}h_n(k_\nu r)\bigg\} - 2rk_\nu^2 h_n(k_\nu r)\\ &\quad + 2(k_\nu r)\bigg\{k_\nu h_n(k_\nu r) - \frac{n+2}{r}h_{n+1}(k_\nu r)\bigg\} + 2k_\nu h_{n+1}(k_\nu r)\\ &\quad - \frac{2}{r}\{(n^2-n)h_n(k_\nu r) - r^2k_\nu^2 h_n(k_\nu r) + 2(k_\nu r)h_{n+1}(k_\nu r)\}\bigg]P_n(\cos\theta)e^{-i\omega t}\\ &= \frac{1}{r^3}\sum_{n=0}^{\infty} C_n(2n+1)i^n S_{\nu n}[\{-n(n^2-n-(k_\nu r)^2)\}h_n(k_\nu r)\\ &\quad + \{(k_\nu r)^3 - (n^2+n+6)(k_\nu r)\}h_{n+1}(k_\nu r)]P_n(\cos\theta)e^{-i\omega t}. \end{aligned} \quad \text{(A10)}$$

By definition,

$$u_r = \frac{\partial\phi}{\partial r} - \bigg[r\nabla^2 - \frac{1}{r}\frac{\partial}{\partial r}r^2\frac{\partial}{\partial r}\bigg]\psi.$$

Now, substituting Eq. (A8) in u_r above, the second term on the right-hand side becomes

$$\bigg[-r\nabla^2 + \frac{1}{r}\frac{\partial}{\partial r}r^2\frac{\partial}{\partial r}\bigg]\psi = -r\nabla^2\psi + \frac{1}{r}\sum_{n=0}^{\infty} C_n(2n+1)i^n S_{\nu n}[n(n+1)h_n(k_\nu r)]P_n(\cos\theta)e^{-i\omega t} - rk_\nu^2\psi. \quad \text{(A11)}$$

The first and third terms on right-hand side in Eq. (A11) combine to yield zero (Helmholtz equation). Therefore, from Eqs. (A4), (A6), and (A11),

$$u_r = \frac{1}{r}\bigg[\sum_{n=0}^{\infty} C_n(2n+1)i^n[\{nj_n(kr) - (kr)j_{n+1}(kr)\} + S_n\{nh_n(kr) - (kr)h_{n+1}(kr)\} + S_{\nu n}\{n(n+1)h_n(k_\nu r)\}]\bigg]P_n(\cos\theta)e^{-i\omega t}. \quad \text{(A12)}$$

Also,

$$u_\theta = \frac{1}{r}\bigg[\sum_{n=0}^{\infty} C_n(2n+1)i^n[j_n(kr) + S_nh_n(kr) + S_{\nu n}\{(n+1)h_n(k_\nu r) - (k_\nu r)h_{n+1}(k_\nu r)\}]\bigg]\frac{\partial}{\partial\theta}[P_n(\cos\theta)]e^{-i\omega t}. \quad \text{(A13)}$$

APPENDIX B: REDUCTION OF THE MONOPOLE RADIATION FORCE FUNCTION TERM IN THE LIMIT OF PARTICLE SIZE MUCH SMALLER THAN THE ACOUSTIC WAVELENGTH

To compute $\beta_0 = \mathrm{Im}(S_0)$, we start from Eq. (29) with $n = 0$ to obtain

$$S_0 = \frac{\begin{vmatrix}-f_{10} & f_{30}\\ -g_{10} & g_{30}\end{vmatrix}}{\begin{vmatrix}f_{20} & f_{30}\\ g_{20} & g_{30}\end{vmatrix}}. \quad \text{(B1)}$$

Using the definitions of f_{1n} through g_{1n} with $n = 0$ and letting $k \to k_0$,

$$\beta_0 = \mathrm{Im}(S_0) = \frac{-j_1(k_0R)y_1(k_0R)}{[j_1(k_0R)]^2 + [y_1(k_0R)]^2}. \quad \text{(B2)}$$

From [30] we know that

$$\begin{aligned} j_1(k_0R) &= \frac{\sin(k_0R)}{(k_0R)^2} - \frac{\cos(k_0R)}{k_0R},\\ y_1(k_0R) &= -\frac{\cos(k_0R)}{(k_0R)^2} - \frac{\sin(k_0R)}{k_0R},\\ [j_1(k_0R)]^2 &+ [y_1(k_0R)]^2 = (k_0R)^{-2} + (k_0R)^{-4}. \end{aligned} \quad \text{(B3)}$$

Also,

$$\begin{aligned} \sin(k_0R) &= k_0R - \frac{(k_0R)^3}{3!} + \cdots,\\ \cos(k_0R) &= 1 - \frac{(k_0R)^2}{2!} + \cdots. \end{aligned} \quad \text{(B4)}$$

Substituting Eqs. (B3) and (B4) in Eq. (B2) and neglecting higher-order terms in k_0R,

$$\beta_0 = -\frac{(k_0R)^3}{3}. \tag{B5}$$

Now substituting Eq. (B5) in Eq. (41), we get

$$\left(Y_{st}^{ff}\right)_M = \tfrac{8}{3}k_0R. \tag{B6}$$

This is identical to $(Y_{st}^{ff})_{M,SB}$ in Eq. (43), if we let $c_p \to \infty$, since we are dealing with rigid particles.

[1] L. V. King, Proc. R. Soc. London Ser. A **147**, 212 (1934).
[2] T. Hasegawa, J. Acoust. Soc. Am. **65**, 32 (1979).
[3] F. G. Mitri and Z. E. A. Fellah, Arch. Appl. Mech. **77**, 1 (2007).
[4] P. Westervelt, J. Acoust. Soc. Am. **23**, 312 (1951).
[5] A. Doinikov, Proc. R. Soc. London Ser. A **447**, 447 (1994).
[6] A. Doinikov, J. Fluid Mech. **267**, 1 (1994).
[7] A. Doinikov, J. Acoust. Soc. Am. **101**, 713 (1997).
[8] A. Doinikov, J. Acoust. Soc. Am. **101**, 722 (1997).
[9] A. Doinikov, J. Acoust. Soc. Am. **101**, 731 (1997).
[10] M. Settnes and H. Bruus, Phys. Rev. E **85**, 016327 (2012).
[11] S. Danilov and M. Mironov, J. Acoust. Soc. Am. **107**, 143 (2000).
[12] F. G. Mitri, New J. Phys. **8**, 138 (2006).
[13] F. G. Mitri and Z. E. A. Fellah, J. Phys. A: Math. Gen. **39**, 6085 (2006).
[14] F. G. Mitri, Ultrasonics **43**, 681 (2005).
[15] H. Bruus, Lab Chip **12**, 1014 (2012).
[16] R. Barnkob, P. Augustsson, T. Laurell, and H. Bruus, Phys. Rev. E **86**, 056307 (2012).
[17] P. Augustsson, R. Barnkob, S. T. Wereley, H. Bruus, and T. Laurell, Lab Chip **11**, 4152 (2011).
[18] M. J. H. Jensen and H. Bruus, J. Acoust. Soc. Am. **133**, 3236 (2013).
[19] P. B. Muller, R. Barnkob, M. J. H. Jensen, and H. Bruus, Lab Chip **12**, 4617 (2012).
[20] L. P. Gorkov, Sov. Phys. Dokl. **6**, 773 (1962).
[21] *Nonlinear Acoustics*, edited by M. F. Hamilton and D. T. Blackstock (Academic, London, 1998).
[22] A. N. Guz, *Dynamics of Compressible Viscous Fluid* (Cambridge Scientific, Cambridge, 2009).
[23] R. Löfstedt and S. Putterman, J. Acoust. Soc. Am. **90**, 2027 (1991).
[24] C. Lee and T. Wang, J. Acoust. Soc. Am. **94**, 1099 (1993).
[25] T. Hasegawa and K. Yosioka, J. Acoust. Soc. Am. **46**, 1139 (1969).
[26] T. Hasegawa and K. Yosioka, J. Acoust. Soc. Am. **58**, 581 (1975).
[27] T. Hasegawa, J. Acoust. Soc. Am. **61**, 1445 (1977).
[28] D. Foresti, M. Nabavi, and D. Poulikakos, J. Fluid Mech. **709**, 581 (2012).
[29] T. Hasegawa, M. Ochi, and K. Matsuzawa, J. Acoust. Soc. Am. **67**, 770 (1980).
[30] NIST Digital Library of Mathematical Functions, Release 1.0.7, http://dlmf.nist.gov/ (online companion to [31]).
[31] *NIST Handbook of Mathematical Functions*, edited by F. W. J. Olver, D. W. Lozier, R. F. Boisvert, and C. W. Clark (Cambridge University Press, New York, 2010).